Microlocal analysis of synthetic aperture radar imaging in the presence of a vertical wall

2008 J. Phys.: Conf. Ser. 124 012025

(http://iopscience.iop.org/1742-6596/124/1/012025)

Journal of Physics: Conference Series **124** (2008) 012025 doi:10.1088/1742-6596/124/1/012025

Microlocal analysis of synthetic aperture radar imaging in the presence of a vertical wall

Romina Gaburro and Clifford Nolan

Department of Mathematics and Statistics, University of Limerick, Castletroy, Ireland

E-mail: romina.gaburro@ul.ie, clifford.nolan@ul.ie

Abstract. We consider the problem of imaging a target located nearby a perfectly reflective vertical wall by making use of a SAR system in the case where a single pass is made over the scene of which we expect to be able to reconstruct a two-dimensional image. Many of the conventional methods make the assumption that the wave has scattered just once from the region to be imaged before returning to the sensor to be recorded. The purpose of this paper is to give a brief idea about how this restriction can be partially removed from a microlocal analysis point of view, in the case where the radar is operating with a poor directivity. The simple case where the antenna is flying perpendicularly to the wall is presented here, while a more in-depth study of this method will be analyzed elsewhere.

1. Introduction

In Synthetic Aperture Radar (SAR) imaging, a plane or a satellite carrying an antenna moves along a flight track. The antenna emits pulses of electromagnetic radiation, which scatter off the terrain and the scattered waves are detected with the same antenna. The received signals are then used to produce an image of the terrain (see [1], [5], [6], [7]).

The nature of the imaging problem depends on the directivity of the antenna. Here we are interested in the case where the antenna has poor directivity and a typical example of that is the foliage-penetrating radar (see [6], [10], [11]), whose low frequencies do not allow for much beam focusing.

We consider the case when the target to be imaged is located nearby a perfectly reflective vertical wall and a single pass along a straight line perpendicular to the wall is made over the scene. The purpose of this paper is to give the reader an understanding of the method used in the case of the most simple setting where the antenna is flying perpendicularly to the vertical wall. In this situation in fact the calculations involved simplify quite a lot and allow perhaps the reader to become more familiar with the tools of microlocal analysis. For a more in-depth analysis of this problem the authors refer to [3].

The data collected depend on two variables, namely the (fast) time variable and the position of the antenna along the flight track (slow variable). Because the data depend on two degrees of freedom, we expect to be able to reconstruct a two-dimensional image of the scene.

The high-frequency deviation of the speed of wave propagation from that in air is known as the ground reflectivity function. The forward scattering operator (by definition) maps the reflectivity function to the scattered waves that are recorded by the same emitting antenna (i.e., the antenna acts as a source and receiver) and it turns out to be a sum of four forward

operators if the target is located in the vicinity of a perfectly reflective vertical wall (see [3], [8]). These correspond to the different paths that the wave can take when scattering to and from the ground. For example the wave may scatter directly to and from the ground or it may first scatter from the wall and then off the ground, etc. To obtain an image, we must backproject the data which means applying a sum of four adjoint scattering operators to the data. This leads to sixteen possible contributions to the image. There is a lot of symmetry and we are able to analyze the resulting image. We show that in the case of poor directivity, it is possible have artifacts in the image. We indicate the relationship between position of the true scatterer and the artifact in the simple setting when the antenna is flying at a fixed height and along a straight line perpendicular to the vertical wall. In the case that one can beam form adequately and direct the beam to a sufficiently small locality on the ground, we show that these artifacts can be avoided.

A weak-scattering approximation is used to model the scattered field which makes the forward scattering operator a linear one. Moreover the operator in question is a Fourier Integral Operator (FIO) (see [2], [4], [8], [9])and so are the four operators which are contributing to it. Such operators map singular distributions to other singular distributions and the relationship between the input and the output singularities forms what is called a canonical relation. Canonical relations associated to FIOs are Lagrangian manifolds and have a rich geometric structure (see [3], [2], [7]). The authors study this in detail for the case when the antenna is flying perpendicularly to a perfectly reflective vertical wall. The outline of the paper is as follows. In section 2, we present a scattering model for the scattering operator in the presence of a vertical wall. This is achieved through the use of method of images ([3]). In section 3 we show the canonical relation is composed of four separate canonical relations. Each one is associated to the different ways in which the wave can scatter between the scene and wall. To obtain an image we compose the adjoint scattering operator with the scattering operator itself. The singularities in the resulting image are analyzed by examining the composition of the canonical relation for the adjoint operator with the canonical relation of the scattering operator. This analysis leads to the results stated in the previous paragraph.

2. The mathematical model of scattering.

2.1. The forward operator

We use the simple scalar wave equation to model the wave propagation

$$\left(\nabla^2 - \frac{1}{c^2(x)}\,\partial_t^2\right)U(t,x) = f, \tag{1}$$

where f denotes the source and the function c is the wave propagation speed. Although the correct model is Maxwell's equations, (1) is commonly used in SAR and represents a good model for sonar and ultrasound for example. As in [3], [8] we make the following assumptions.

Assumption 1. *We assume that the target is well separated from the region where the sensors are located and that in the intervening region $c(x) = c_0$, where c_0 is the (assumed constant) speed of light in air.*

Assumption 2. *We assume that the target to be imaged is a-priori known to lie on the ground and lies strictly on one (known) side of a vertical wall. We assume that the ground is locally flat, so if we denote by (x_1, x_2, x_3) the cartesian coordinates in $\mathbb{R}^3$, then the ground can be locally identified with $\mathbb{R}^2 = \{(x_1,\, x_2,\, 0) \mid x_i \in \mathbb{R},\, i = 1,\, 2\} \subseteq \mathbb{R}^3$.*
The vertical wall can be taken for simplicity as the infinite vertical plane $x_1 = 0$ so we can identify the area to be imaged by the set $\mathbb{R}^2_+ = \{(x_1,\, x_2,\, 0) \mid x_i \in \mathbb{R},\, i = 1,\, 2,\, x_1 > 0\}$.

We denote by

$$\Gamma_+ := \left\{ \mathbf{\Gamma}_+(s) \;\middle|\; s^{min} < s < s^{max} \right\}$$

the straight line along which the antenna is moving along (flight track).

There are four ways for the wave to hit the target on the ground and return to the antenna. Indeed the wave may scatter directly to and from the target. Or, the wave may scatter first from the wall, then from the target and finally back to the antenna. The third means of scattering is the reverse of the former and finally, the last method involves scattering from the wall on the way down to the target and again on the way back to the antenna. The data that is collected contains all four kinds of scattering events in it. See Figure 1 for an illustration of this.

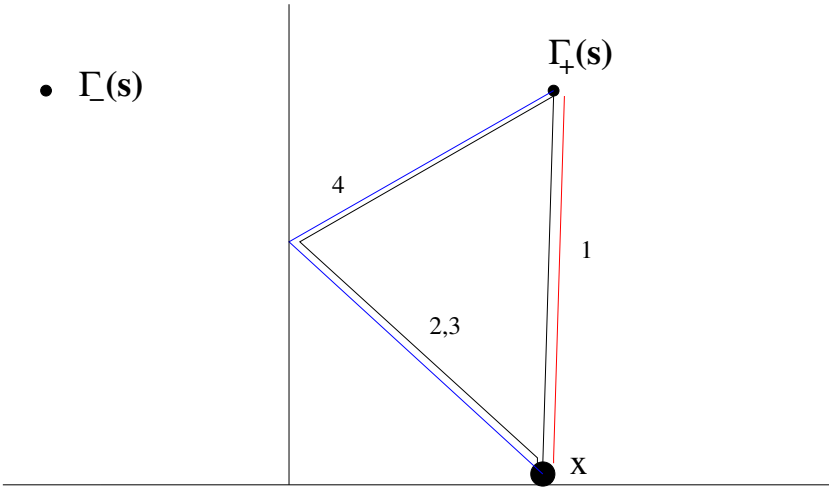

Figure 1. In case 1, the wave scatters directly to and from the target. In case 2, the wave scatters from the wall to the target and back to the receiver. In case 3, the wave scatters from the target to the wall and back to the receiver. Finally, in case 4, the wave scatters to the wall to the target and back to the wall again before returning to the receiver.

We represent the (perfectly reflecting) wall via the method of images, by placing a virtual source at $\Gamma_-(s)$ symmetrically on the other side of the wall from the actual source location ($\Gamma_+(s)$) (see [3], [8]). Note that the argument s in $\Gamma_\pm(s)$ denotes the current real (+ subscript) and virtual source position (− subscript) respectively, as it is moved over a path parametrized by s.

Let us recall that the scattering region is $\mathbb{R}^2_+$, the data space parameters are $(s^{min},\ s^{max}) \times [0,\ T]$ and introduce the *reflectivity function* $V(x) = \frac{1}{c_0^2} - \frac{1}{c^2(x)}$, which encodes rapid changes in material properties. For example, when the radio wave impinges on a building on the ground, the propagation speed changes suddenly, according to the building materials.
Then the *scattering operator* F from "scene" $V(x)$ at the point $x \in \mathbb{R}^2_+$ to the collected data $d(s,\ t)$ at the time $t \in [0,\ T]$ and location s (i.e at the antenna location $\Gamma_+(s)$) is given by

$$\begin{aligned} d(s,\,t) = FV(s,\,t) &= \int e^{-i\omega\left(t-2|z-\Gamma_+(s)|/c_0\right)}\, a_1(x,\,s,\,t,\,\omega)\, V(z)\, d\omega\, dz \\ &- \int e^{-i\omega\left(t-(|z-\Gamma_+(s)|+|z-\Gamma_-(s)|)/c_0\right)}\, a_2(x,\,s,\,t,\,\omega)\, V(z)\, d\omega\, dz \\ &- \int e^{-i\omega\left(t-(|z-\Gamma_+(s)|+|z-\Gamma_-(s)|)/c_0\right)}\, a_3(x,\,s,\,t,\,\omega)\, V(z)\, d\omega\, dz \\ &+ \int e^{-i\omega\left(t-2|z-\Gamma_-(s)|/c_0\right)}\, a_4(x,\,s,\,t,\,\omega)\, V(z)\, d\omega\, dz \\ &:= F_1\, V(s,\,t) + F_2\, V(s,\,t) + F_3\, V(s,\,t) + F_4\, V(s,\,t). \end{aligned} \tag{2}$$

The amplitudes $a_i, i = 1, \ldots 4$ are geometrical optics amplitudes, and encode the geometrical spreading, beam pattern, etc, for the emitted and measured waves, therefore they are known quantities. For more detail on this we refer to [3]. We wish to reconstruct the unknown function V from the data d, i.e., solve an inverse problem.

2.2. Statement of the inverse problem

The idealized inverse problem consists in determining V from the knowledge of $d(s,\,t)$, for any $(s,\,t) \in [s^{min},\,s^{max}] \times [0,\,T]$, for some T. The amplitudes a_i, $i = 1 \ldots 4$ appearing in (2) reflect the four ways for the wave to scatter on its way from the source to the target and back to the receiver location again.

For technical reasons, we need to assume

Assumption 3. *For $1 \le j \le 4$, the amplitude a_j satisfies*

$$\sup_{(s,\,t,\,x)\in K} |\, \partial_\omega^\alpha\, \partial_s^\beta\, \partial_t^\delta\, \partial_x^\rho\, a_j(x,\,s,\,t,\,\omega)\, | \le C^j_{K,\,\alpha,\,\beta,\,\delta,\,\rho}(1+\omega^2)^{(2-|\alpha|)/2}, \tag{3}$$

where K is any compact set in $[s_{min}, s_{max}] \times [0,T] \times \mathbb{R}^2_+$ and α, β, δ, ρ are arbitrary multi-indices of the appropriate dimension.

The above assumption is valid for example when the waveform sent to the antenna is approximately a delta function and the antenna is sufficiently broadband (see [3], [5]). Note that the coefficients $C^j_{K,\,\alpha,\,\beta,\,\delta,\,\rho}$ are constants depending only on their indices.

Assumption 3 implies that the forward operators $F_j, 1 \le j \le 4$ are Fourier Integral Operators (FIOs) (see [2], [3], [4], [8], [9]).

3. Analysis of the scattering operator

3.1. Fourier Integral Operators (FIOs)

We saw in section 2 that $F_i, 1 \le i \le 4$ is a FIO and standard arguments in FIO theory give us information about how $F_i, 1 \le i \le 4$ maps singularities from the scene into the data. We will review this below, and to begin with, we recall the following

DEFINITION 3.1. *Let $\mathcal{X} = \mathbb{R}^2_+$, $\mathcal{Y} = (s^{min},\, s^{max}) \times [0,\, T]$, $\mathcal{E}'(\mathcal{X})$, $\mathcal{E}'(\mathcal{Y})$ be the spaces of distributions with compact support in $\mathcal{X}$ and $\mathcal{Y}$ respectively. If F is a Fourier Integral Operator*

$$F : \mathcal{E}'(\mathcal{X}) \longrightarrow \mathcal{E}'(\mathcal{Y})$$

given by the oscillatory integral

$$Fu(y) = \int e^{i\phi(y,\,x,\,\omega)}\, a(y,\,x,\,\omega)\, u(x)\, d\omega\, dx, \tag{4}$$

for any $u \in \mathcal{E}'(\mathcal{X})$, then its (twisted) ***canonical relation*** *is the set*

$$\begin{aligned}\Lambda'_F =&\Big\{\big((y,\,\eta),\,(x,\,\xi)\big) \in T^\star(\mathcal{Y}\times\mathcal{X})\setminus\{0\} \;\mid\; (y,\,x,\,\omega)\in C_\phi \cap \mathrm{EssSupp}(a),\\ &\eta = D_y\phi(y,\,x,\,\omega),\,\xi = -D_x\phi(y,\,x,\,\omega)\Big\},\end{aligned} \tag{5}$$

where D_x and D_y denote the gradients with respect to the x and y variable respectively and $\{0\}$ is the zero section of $T^*(\mathcal{X}\times\mathcal{Y})$. The set C_ϕ is defined as the critical set points

$$C_\phi = \big\{(y,\,x,\,\omega) \;\mid\; D_\omega\phi(y,\,x,\,\omega) = 0\big\}, \tag{6}$$

which is called the ***critical manifold****, and* EssSupp*(a) is defined via its complement:*

$$\begin{aligned}{}^{\mathcal{C}}\mathrm{EssSupp}(a) =&\{(y,\,x,\,\omega) \;\mid\; a(y,x,\omega) \text{ and its derivatives decrease faster}\\ &\text{than any negative power of } \omega, \text{ as } \mid\omega\mid\to\infty\}.\end{aligned}$$

Note that the frequency ω can be multi-dimensional.

DEFINITION 3.2. *If we denote by $\mathcal{D}'(\mathcal{X})$ the set of distributions on $\mathcal{X}$ and if $u\in\mathcal{D}'(\mathcal{X})$, then the* ***wave front set*** $\mathbf{WF(u)}$ *of u is defined as the complement in $T^\star\mathcal{X}\setminus\{0\}$ of the collection of all $(x,\,\xi)\in T^\star\mathcal{X}\setminus\{0\}$ such that there exists a neighborhood U of x and a neighborhood $\mathcal{U}$ of ξ such that for any $\varphi\in C_0^\infty(U)$, with $x\in supp(\varphi)$ and any $N\in\mathbb{N}$:*

$$\mathcal{F}(\varphi\,u)(\tau\xi) = O(\tau^{-N}), \qquad \text{for} \quad \tau\to\infty, \quad \text{uniformly in} \quad \xi\in\mathcal{U}.$$

Here $\mathcal{F}(\varphi\,u)$ denotes the Fourier transform of $\varphi\,u$.

WF(u) is a closed cone in $T^\star\mathcal{X}\setminus\{0\}$ and its singular support satisfies $\mathrm{singsupp}(u) = \pi\big(WF(u)\big)$, where π is the natural projection of $T^\star\mathcal{X}\setminus\{0\}$ into $\mathcal{X}$ (see [2]).

DEFINITION 3.3. *If F is given by* (4) *with distributional kernel $K_F\in\mathcal{D}'(\mathcal{Y}\times\mathcal{X})$ given by the oscillatory integral*

$$K_F(y,\,x) = \int e^{i\phi(y,\,x,\,\omega)}a(y,\,x,\,\omega)\,d\omega,$$

the ***wavefront relation*** $\mathbf{WF'(F)}$ *is defined by*

$$WF'(F) = \Big\{\big((y,\,\eta),\,(x,\,\xi)\big)\in T^\star(\mathcal{Y}\times\mathcal{X})\setminus\{0\} \mid (y,\,x,\,\eta,\,-\xi)\in WF(K_F)\Big\}.$$

It turns out (see [2]) that

$$\begin{aligned}WF(Fu)&\subseteq WF'(F)\circ WF(u)\\ WF'(F)&\subseteq \Lambda'_F,\end{aligned} \tag{7}$$

where"$\circ$" stands for the following composition

$$WF'(F)\circ WF(u) = \{\;(y,\eta)\mid \exists\;((y,\eta),(x,\xi))\in WF'(F),\;(x,\xi)\in WF(u)\;\}. \tag{8}$$

Let us compute the canonical relations $\Lambda'_{F_i}, 1\le i\le 4$. Note that $\Lambda'_{F_2} = \Lambda'_{F_3}$, so we will only compute $\Lambda'_{F_i}, i = 1,2,4$.

3.2. The canonical relations
We start by making the following assumption.

Assumption 4. *The antenna is flying perpendicular to the wall $x_1 = 0$ at constant height h, i.e.*

$$\begin{aligned}\Gamma_+(s) &= (\gamma_1(s),\, 0,\, h) = (\gamma_1,\, 0,\, h)\\ \Gamma_-(s) &= (-\gamma_1(s),\, 0,\, h) = (-\gamma_1,\, 0,\, h),\end{aligned}$$

so that with arc length as the parametrisation, the real and the virtual velocity fields are as follows

$$\begin{aligned}\dot\Gamma_+(s) &:= V_+ = (1,\, 0,\, 0)\\ \dot\Gamma_-(s) &:= V_- = (-1,\, 0,\, 0),\end{aligned}$$

where $\dot\Gamma$ denotes the derivative of Γ with respect to s.

With appropriate time units, we may take $c_0 = 1$. Define

$$R_+ := \left[(x_1-\gamma_1)^2 + x_2^2 + h^2\right]^{1/2} =\mid x - \Gamma_+(s) \mid \tag{9}$$

$$R_- := \left[(x_1+\gamma_1)^2 + x_2^2 + h^2\right]^{1/2} =\mid x - \Gamma_-(s) \mid \tag{10}$$

so that the (twisted) canonical relations $\Lambda'_{F_i}, 1 \le i \le 4$ associated to the operators F_i, $1 \le i \le 4$ are respectively (see [3])

$$\begin{aligned}\Lambda'_{F_1} = \Big\{ & \big((s,\, t,\, \sigma,\, \tau),\, (x,\, \xi)\big) \mid\ t = 2\, R_+;\\ & \sigma = 2\tau \frac{x_1-\gamma_1}{R_+};\\ & \tau = -\omega;\\ & \xi = -2\tau(x - \widehat{\Gamma_+}(s))\Big\};\end{aligned} \tag{11}$$

$$\begin{aligned}\Lambda'_{F_2} = \Big\{ & \big((s,\, t,\, \sigma,\, \tau),\, (x,\, \xi)\big) \mid\ t = (R_+ + R_-);\\ & \sigma = \tau\Big(\frac{x_1-\gamma_1}{R_+} - \frac{x_1+\gamma_1}{R_-}\Big);\\ & \tau = -\omega;\\ & \xi = -\tau\Big((x - \widehat{\Gamma_+}(s)) + (x - \widehat{\Gamma_-}(s))\Big)\Big\};\end{aligned} \tag{12}$$

$$\begin{aligned}\Lambda'_{F_4} = \Big\{ & \big((s,\, t,\, \sigma,\, \tau),\, (x,\, \xi)\big) \mid\ t = 2\, R_-;\\ & \sigma = -2\tau \frac{x_1+\gamma_1}{R_-};\\ & \tau = -\omega;\\ & \xi = -2\tau(x - \widehat{\Gamma_-}(s))\Big\},\end{aligned} \tag{13}$$

where for any non-zero vector $v \in \mathbb{R}^3$, we denote by $|v|$ its *length* (i.e. its Euclidean norm) and we define $\hat{v} = \frac{v}{|v|}$.

Forming an image usually involves operating on the data with a weighted adjoint operator (the reason for this will become clear soon). The forward map is given by the four contributions

$$F = F_1 + F_2 + F_3 + F_4$$

and the adjoint of F, $F^\star$ by

$$F^\star = F_1^\star + F_2^\star + F_3^\star + F_4^\star,$$

where $F_i^\star$ is the adjoint of F_i. Singularities in the scene will be mapped into singularities in the data by any of the F_i, while singularities in the data will be mapped into singularities in the scene by the adjoint maps $F_i^\star$.

Our goal is to analyse the resulting image, determine which kind of artifacts it may contain, and see if we can avoid them. To do so, we will see that we need to analyse the composition of the (twisted) canonical relations

$$\Lambda'_{F_i^\star} \circ \Lambda'_{F_j}, \qquad \text{for any} \quad 1 \leq i, j \leq 4, \tag{14}$$

where

$$\Lambda'_{F_i^\star} = {}^t\Lambda'_{F_i}, \qquad \text{for any} \quad 1 \leq i \leq 4,$$

and the superscript t denotes the transposed relation.

The reason for this is that if we denote by I the reconstructed image, FIO theory implies

$$\begin{aligned} WF(I) &\subseteq WF'(F^\star) \circ WF'(F) \circ WF(V) \\ &\subseteq \left(\bigcup_{i,j=1}^{4} \Lambda_i'^\star \circ \Lambda'_j \right) \circ WF(V). \end{aligned} \tag{15}$$

Compositions in (14) and (15) are meant as compositions of relations, i.e. if $\mathcal{R}_1 \subset U \times V$, $\mathcal{R}_2 \subset V \times W$ are relations, then the *composition* $\mathcal{R}_1 \circ \mathcal{R}_2 \subset U \times W$ is defined by

$$\mathcal{R}_1 \circ \mathcal{R}_2 = \big\{(u, w) \in U \times W;\ \exists v \in V : (u, v) \in \mathcal{R}_1 \text{ and } (v, w) \in \mathcal{R}_2\big\}.$$

For any i, $j = 1, \ldots, 4$, we will sometimes refer in the sequel to the *case* or *pair* $(i,\ j)$ or speak about *interaction between experiments i and j* by meaning we are analysing the object $\Lambda'_{F_i^\star} \circ \Lambda'_{F_j}$ (or similarly $\Lambda'_{F_j^\star} \circ \Lambda'_{F_i}$) and we will call it *backprojection* (of the data).

3.3. Analysis of the diagonal terms.

We need only analyze $\Lambda'_{F_2^\star} \circ \Lambda'_{F_2}$ (pair (2, 2)) among the diagonal compositions in (14) as pair (1, 1)(and similarly (4, 4)) have been studied in [5], while case (3, 3) is very similar to (2, 2). Let us denote by $x = (x_1, x_2, 0)$ a point on the ground. By defining the quantity

$$p := \frac{\sigma}{\tau}, \tag{16}$$

and recalling (12) we have

$$\frac{x_1-\gamma_1}{R_+}-\frac{x_1+\gamma_1}{R_-}=p \tag{17}$$

$$R_+ + R_- = t. \tag{18}$$

Notice that the travel time condition given by (18) describes for any s and t the intersection of an ellipsoid (whose foci are $\Gamma_+(s), \Gamma_-(s)$) with the earth's surface. In our specific case, where the earth is locally flat, this intersection is an ellipse. The equation of this ellipse can be obtained by squaring (18) a couple of times and rearranging to get

$$x_2^2 = \Big(\frac{t^2}{4}-\gamma_1^2-h^2\Big)+\Big(\frac{4\gamma_1^2}{t^2}-1\Big)x_1^2. \tag{19}$$

One can directly verify the identity

$$4\gamma_1 x_1 = R_-^2 - R_+^2 \tag{20}$$

and by substituting $R_- = t - R_+$ in the latter equation and rearranging it we obtain

$$x_1 = \frac{t}{4\gamma_1}\big(t-2R_+\big). \tag{21}$$

Substituting (21) into (17) we obtain the following quadratic equation for R_+

$$R_+^2 - tR_+ + \frac{\alpha}{4} = 0, \tag{22}$$

with

$$\alpha = \frac{t(t^2-4\gamma_1^2)}{(t+p\gamma_1)}, \tag{23}$$

giving two possible solutions

$$R_+ = \frac{t \pm (t^2-\alpha)^{1/2}}{2},$$

but $R_+ < t/2$, which leaves the unique solution

$$R_+ = \frac{t-(t^2-\alpha)^{1/2}}{2}. \tag{24}$$

By (24) and (21) we finally get

$$x_1 = \frac{t(t^2-\alpha)^{1/2}}{4\gamma_1}, \tag{25}$$

so that x_1 is uniquely determined. If we operate the radar in side-scan mode, i.e. we illuminate only one side of the projected flight path on the ground, x_2 is uniquely determined (no sign ambiguity) by (19), and since $x_3 = 0$ for a scatterer on the ground, we have that the scatterer location x is determined. This shows that there are no artifacts present in the image obtained from experiment 2, in the case when the radar is operated in side-scan mode.

Remark 3.1. *(See [3])*

$$0 < \alpha < t^2. \tag{26}$$

The latter inequality guarantees a real root in (25).

3.3.1. Analysis of the non-diagonal terms. We analyze the relations $\Lambda'_{F_i^*} \circ \Lambda'_{F_j^*}$ for $i \neq j$ in this subsection. Again we assume that the antenna is flying perpendicularly to the wall i.e. Assumption 4 holds. In that case we have

$$\sigma_1 = \frac{2\tau}{c_0} \frac{x_1 - \gamma_1}{R_+} \tag{27}$$

$$\sigma_2 = \sigma_3 = \frac{\tau}{c_0} \left(\frac{x_1 - \gamma_1}{R_+} - \frac{x_1 + \gamma_1}{R_-} \right) \tag{28}$$

$$\sigma_4 = -\frac{2\tau}{c_0} \frac{x_1 + \gamma_1}{R_-}. \tag{29}$$

Notice that

$$\sigma_1 \mid_{x_1=0} = \sigma_2 \mid_{x_1=0} = \sigma_3 \mid_{x_1=0} = \sigma_4 \mid_{x_1=0} = -\frac{2\tau}{c_0} \frac{\gamma_1}{R_+ \mid_{x_1=0}} < 0$$

and

$$\lim_{x_1 \to \infty} \sigma_1(x) = \frac{2\tau}{c_0}; \quad \lim_{x_1 \to \infty} \sigma_2(x) = \lim_{x_1 \to \infty} \sigma_3(x) = 0; \quad \lim_{x_1 \to \infty} \sigma_4(x) = -\frac{2\tau}{c_0}.$$

Moreover

$$\partial_{x_1} R_+ = R_+^{-1}(x_1 - \gamma_1) \tag{30}$$

$$\partial_{x_1} R_- = R_-^{-1}(x_1 + \gamma_1) \tag{31}$$

and

$$\begin{aligned} \partial_{x_1}\sigma_1 &= \frac{2\tau}{c_0} \frac{R_+ - (x_1 - \gamma_1)\partial_{x_1} R_+}{R_+^2} \\ &= \frac{2\tau}{c_0} \frac{R_+^2 - (x_1 - \gamma_1)^2}{R_+^3} \end{aligned} \tag{32}$$

$$\begin{aligned} \partial_{x_1}\sigma_2 &= \partial_{x_1}\sigma_3 = \frac{\tau}{c_0} \left\{ \frac{R_+ - (x_1 - \gamma_1)\partial_{x_1} R_+}{R_+^2} - \frac{R_+^2 - (x_1 - \gamma_1)^2}{R_+^3} \right\} \\ &= \frac{\tau}{c_0} \frac{(x_2^2 + h^2)(R_-^3 - R_+^3)}{(R_+ R_-)^3} \end{aligned} \tag{33}$$

$$\begin{aligned} \partial_{x_1}\sigma_4 &= \frac{2\tau}{c_0} \frac{R_- - (x_1 - \gamma_1)\partial_{x_1} R_-}{R_-^2} \\ &= -\frac{2\tau}{c_0} \frac{R_-^2 - (x_1 + \gamma_1)^2}{R_-^3}. \end{aligned} \tag{34}$$

By (9), (10) we have that $R_+ > (x_1 - \gamma_1)$ and $R_- > (x_1 + \gamma_1)$, which imply that $\partial_{x_1}\sigma_1 > 0$ and $\partial_{x_1}\sigma_4 < 0$, respectively, i.e. σ_1 is increasing and σ_4 is decreasing in the x_1-direction. Moreover $R_- > R_+ > 0$ as the target is located on the right hand side of the vertical wall $x_1 = 0$, which implies that $\partial_{x_1}\sigma_2 > 0$, $\partial_{x_1}\sigma_3 > 0$, i.e. σ_2, σ_3 are increasing in the x_1-direction. Therefore, it's impossible to get a common value between σ_1 and σ_4 and between σ_2 or σ_3 and σ_4. We can therefore conclude that the composition in (14) is empty for the pairs

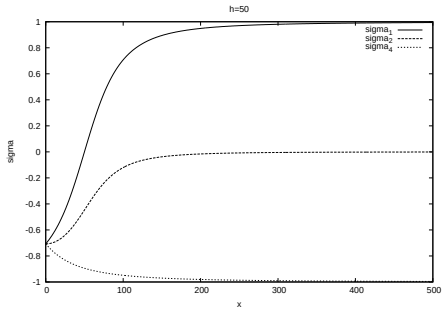

Figure 2. Figure shows the graph of σ_1, σ_2 and σ_4 when the antenna is flying on a straight line perpendicular to the wall, at the fixed height of $h = 50$ and the source location is $\Gamma_+ = (50, 250, 50)$

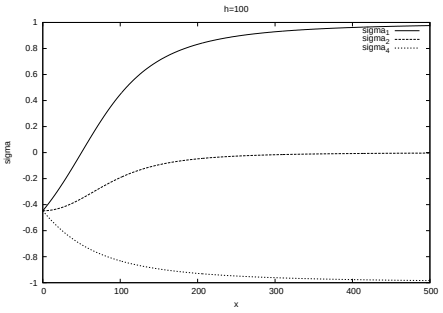

Figure 3. Figure shows the graph of σ_1, σ_2 and σ_4 when the antenna is flying on a straight line perpendicular to the wall, at the fixed height of $h = 100$ and the source location is $\Gamma_+ = (50,\ 250,\ 100)$

$(i, j) = (1, 4), (4, 1), (2, 4), (4, 2), (3, 4), (4, 3)$ (see Figures 2 and 3).

Let us consider pairs $(i, j) = (1, 2), (2, 1)$. Cases $(i, j) = (1, 3), (3, 1)$ can be treated in a similar way. We assume again that Assumption 4 holds and we denote by $x = (x_1, x_2, 0)$ and $z = (z_1, z_2, 0)$ two points on the ground. In order to compose $\Lambda_{F_1^*} \circ \Lambda_{F_2}$ (or similarly $\Lambda_{F_2^*} \circ \Lambda_{F_1}$) at points x, z we must have (for coincidence of σ values)

$$2\,\frac{z_1 - \gamma_1}{R^z_+} = \left(\frac{x_1 - \gamma_1}{R^x_+} - \frac{x_1 + \gamma_1}{R^x_-}\right), \tag{35}$$

moreover x, z must satisfy the two travel time conditions respectively

$$R^x_+ + R^x_- = t \tag{36}$$
$$2R^z_+ = t, \tag{37}$$

where we have used the notation R^x_+ for R_+ defined in (9) for the scattering point x and R^z_+ when the scattering point x is replaced by z, etc.
By combining (35), (36) and (37) we obtain

$$t(t - R^x_+)(x_1 - \gamma_1) - tR^x_+(x_1 + \gamma_1) = 4R^P_+(t - R^x_+)(z_1 - \gamma_1) \tag{38}$$

from which we extract the following expression for z_1 as a function of x

$$z_1 = \Big[\big(4(R^x_+)^2 + t^2 - 4tR^x_+\big)\gamma_1 + \big(2tR^x_+ - t^2\big)x_1\Big]/4((R^x_+)^2 - tR^x_+). \tag{39}$$

Using equations (22) and (24), it follows that

$$z_1 = \left(\frac{t^2 - \alpha}{4\gamma_1\alpha}\right)\ \left(t^2 - 4\gamma_1^2\right), \tag{40}$$

which in turn implies that

$$z_1 - x_1 = \left[(t^2-\alpha)(t^2-4\gamma_1^2)/\alpha - t(t^2-\alpha)^1/2\right]/\alpha. \tag{41}$$

The above formula gives us the relation between the first component x_1 and z_1 of two points on the ground (scene) $x = (x_1,\, x_2,\, 0)$ and $z = (z_1,\, zeta,\, 0)$ such that

$$\Big(\big(x,\, \xi\big),\, \big(z,\, \zeta\big)\Big) \in \Lambda_{F_1^*} \circ \Lambda_{F_2}$$

(or similarly $\Big(\big(z,\, \zeta\big),\, \big(x,\, \xi\big)\Big) \in \Lambda_{F_2^*} \circ \Lambda_{F_1}$). Such points x, z are therefore the images obtained by backprojecting the same data, therefore one of them (say x) must be the real scatterer and the other one must be an artifact.

Note that α (defined in (23)) is a function of p, which is a function of x_1. Therefore, (41) gives us a formula for the distance between z_1 and x_1 in terms of x_1. It follows that if we want to avoid artifacts resulting from backprojecting with (possibly weighted) operators $F_i^*, i = 1, 2$, we must ensure that the beam width in the first coordinate direction is smaller than that predicted by the right hand side of (41). Note that this implies a variable beam width restriction, which depends on the (x_1) location that is being illuminated for imaging. This beam forming can be done synthetically and it therefore does not impose extra logistical difficulties in acquiring the data. We can in fact superimpose the signals coming from each component of the antenna array to constructively and destructively interfere at particular locations on the ground. This can be done synthetically, without the need to physically beam form at the time of the experiment.
If the required beam forming is not possible, then artifacts will be present and their location can be predicted by equation (41) in conjunction with (37), i.e., by intersecting a line with a circle on the ground. Of course, this may not be a complete determination if the usual left-right ambiguity of radar is still present (due to not being able to operate in side-scan mode).

Acknowledgments

RG and CN acknowledge the support of Science Foundation Ireland (Grant 03/IN3/I401). RG would also like to acknowledge the financial support of the Mathematics Applications Consortium for Science and Industry (MACSI: www.macsi.ie) funded under the Science Foundation Ireland Mathematics Initiative 06/MI/005.

References

[1] Cheney M 2001 A mathematical tutorial on synthetic aperture radar *SIAM Review* **43** pp 301-12
[2] Duistermaat J J 1996 *Fourier Integral Operators* (Boston: Birkhauser)
[3] Gaburro R and Nolan C J 2007 Enhanced imaging from multiply scattered waves, to appear in *Inverse Problems and Imaging*.
[4] Grigis A and Sjöstrand J 1994 *Microlocal Analysis for Differential Operators: An Introduction (London Mathematical Society Lecture Note Series)* vol 196 (Cambridge: Cambridge University Press)
[5] Nolan C J and Cheney M 2002 Synthetic aperture inversion *Inverse Problems* **18** pp 221-36
[6] Nolan C J and Cheney M 2003 Synthetic aperture inversion for arbitrary flight paths and non-flat topography *IEEE Trans. on Image Processing* **12** pp 1035-43
[7] Nolan C J and Cheney M 2004 Microlocal analysis of synthetic aperture radar imaging *J. Fourier Analysis and its Applications* **10** pp 133-48
[8] Nolan C J, Cheney M, Dowling T and Gaburro R 2006 Enhanced angular resolution from multiply scattered waves *Inverse Problems* **22** pp. 1817-34
[9] Treves F 1980 *Introduction to Pseudodifferential and Fourier Integral Operators* vol 1 and 2 (New York: Plenum Press)
[10] Ulander L M H and Frölund P O 1998 Ultra-wideband SAR interferometry *IEEE Trans. Geosci.Remote Sensing* **36** pp 1540-50
[11] Ulander L M H and Hellsten H 1999 Low-frequency ultra-wideband array-antenna SAR for stationary and moving target imaging, *Conf. SPIE 13th Annuual Int. Symp on Aerosense* Orlando FL